RESEARCH PAPER

Comprehensive characterization and simultaneous analysis of overall lipids in reconstructed human epidermis using NPLC/HR-MSⁿ: 1-O-E (EO) Cer, a new ceramide subclass

Ali Assi[1] · Joudi Bakar[1] · Danielle Libong[1] · Elie Sarkees[1] · Audrey Solgadi[2] · Arlette Baillet-Guffroy[1] · Rime Michael-Jubeli[1] · Ali Tfayli[1]

Abstract

Stratum corneum lipids are responsible for the skin's barrier function. They are the final product of epidermis lipid biosynthesis. During this process, lipids evolve from simple to complex structures in three main levels respectively (*stratum basal level*, *stratum granulosum level*, and *stratum corneum level*). Our aim was to simultaneously analyze and characterize the structure of total epidermis lipids. A powerful analytical method (normal-phase liquid chromatography coupled with high-resolution mass spectrometry (NPLC/HR-MSⁿ)) was developed in order to separate, in a single run, lipid classes with a wide polarity range. Chromatographic conditions were particularly designed to analyze lipids of intermediate polarity such as ceramides. Rich information was obtained about the molecular structure of keratinocyte differentiation biomarkers such as ceramides, glucosylceramides, and sphingomyelins and the microstructures of reconstructed human epidermis lipids using HR-MSⁿ. A new subclass of ceramides, 1-O-Acyl Omega-linoleoyloxy ceramides [1-O-E (EO) Cer] has been highlighted. This class is double esterified on the 1-O-position of sphingoid base with long to very long chain acyl residues (1-O-E) and on the position of ω-hydroxyl group of fatty acid with the linolenic acid (EO). Considering its chemical structure and hydrophobicity, this subclass can contribute to the skin barrier. In addition, we detected a new epidermis sphingomyelins. Our lipidomic approach offers a direct access to epidermis biomarkers.

Keywords 1-O-E (EO) Cer · Ceramides · Glucosylceramides · Sphingomyelins · Reconstructed human epidermis · NPLC/HR-MSⁿ

Abbreviations

APCI	Atmospheric pressure chemical ionization
APPI	Atmospheric pressure photoionization
CER	Ceramide
ESI	Electrospray ionization
FFA	Free fatty acid
GlcCER	Glucosylceramide
HPLC	High-performance liquid chromatography
HR-MS	High-resolution mass spectrometry
LA	Linoleic acid
NPLC	Normal-phase liquid chromatography
RHE	Reconstructed human epidermis
RP-LC	Reversed-phase liquid chromatography
SC	*Stratum corneum*
SM	Sphingomyelin
Sph	Sphingoid base moiety
ULC	Ultra-long chain

Ali Assi and Joudi Bakar contributed equally to this work.

✉ Rime Michael-Jubeli
  rime.michael-jubeli@u-psud.fr

[1] Lip(Sys)2, Chimie Analytique Pharmaceutique (FKA EA4041 Groupe de Chimie Analytique de Paris-Sud), Université Paris-Sud, Université Paris-Saclay, 92290 Châtenay-Malabry, France

[2] SAMM, UMS IPSIT, Université Paris Sud, Université Paris-Saclay, 92290 Chatenay-Malabry, France

Introduction

The epidermis is the upper layer of the three main skin layers: hypodermis, dermis, and epidermis [1]. It acts as a protective barrier against water loss and eliminates foreign substances and micro-organisms [2]. The barrier function strongly relies

Ⓐ Springer

on the outermost layer of the epidermis, the *stratum corneum* (SC) [3]. The SC is composed of three major components: corneocytes, corneodesmosomes, and an intercellular lipid matrix [4] which is responsible for the formation and maintenance of the skin barrier [5–7]. The major lipid classes in human's SC are cholesterol, free fatty acids, and ceramides (CERs). Ceramides are essential to maintain the integrity of the skin barrier and the epidermis hydration [8].

Since various ceramide species and metabolites have well-recognized roles in signaling different cellular outcomes, such as proliferation, differentiation, and/or apoptosis, therefore, it is increasingly important to understand how the production and the function of ceramides are controlled in the epidermis. Reduced levels of epidermal ceramides have been linked to water loss and barrier dysfunction [9]. Conversely, inappropriate accumulation of some ceramides leads to keratinocyte's death and alteration of barrier function [10, 11]. These observations indicate that the balance of ceramide metabolism plays a major role in the state of the skin barrier. Ceramides are synthetized from keratinocytes by de novo pathway. At the level of germinative cells, newly synthesized CERs are immediately converted to glucosylceramides (GlcCERs) and sphingomyelins (SM). These molecules are then packaged in single secretory lamellar bodies (LB), which their quantities increase in the later stages of keratinocyte differentiation. GlcCERs and SMs are transported and secreted at the interface of *stratum granulosum* and *stratum corneum*, where they are respectively hydrolyzed by beta-glucocerebrosidase and sphingomyelinase and then converted to CERs [9]. These elements are mostly known at the level of lipid classes but remain unclear at their structural microheterogeneity. However, the variations in compactness of intercorneocyte lipids observed during ageing and in several skin diseases are correlated with the structural microheterogeneity of ceramides [12–14].

Our aim is to develop an analytical method to separate the epidermis lipid classes in a single run and to characterize three main lipid classes: ceramides, glucosylceramides, and sphingomyelins at a molecular level, in order to follow—in further studies—the evolution of these lipids during the keratinocyte differentiation through all epidermis layers. In fact, these three classes are considered to be the biomarkers of the principal steps of the epidermis lipid biosynthesis.

Numerous analytical advances [15–17] have been made in the past few years allowing the separation and the characterization of these epidermal lipids but often they are limited to lipid classes and subclasses, which differed by the number and/or position of the hydroxylation, the length and/or number of fatty acid chain, and the number and position of the unsaturation. In addition to the large difference in the polarity between the classes and the large number of molecules, the structural microheterogeneity within each class or subclass can be considered a source of complexity in the characterization of such a lipid mixture.

Although several studies have established an analytical method of total lipids [18], our analytical method is specific to the epidermis lipidome: free fatty acids, cholesterol, glycerides, ceramides, glucosylceramides, sphingomyelins, and phospholipids. The particularity of this lipidome is that the majority of the lipid classes are ceramides. This class can be composed by fifteen subclasses based on the polarity of the polar head. In contrast of ceramides found in other body regions, ceramides in the *stratum corneum* have a wide variety of structures [19, 20]. A ceramide is composed of a sphingoid base and a fatty acid [21, 22]. In human SC, the CERs differ from each other in the architecture of the polar head group, the length of the acyl chain, and their unsaturations. They can be subdivided into five groups based on sphingoid base: dihydrosphingosine (DS), sphingosine (S), phytosphingosine (P), 6-hydroxysphingosine (H), or the dihydroxy-dihydro sphingosine (T) [23, 24]. Regarding the part of fatty acids, the acyl chain is a non-hydroxy (N), α-hydroxy (A), or ω-hydroxy (O) [25]. The latter class, esterified ULC-ceramides, represents a distinctive class of skin ceramides, and derived from esterification (E) of the ω-hydroxyl group of the ULC fatty acid moiety (O) [21, 26–28]. These ceramides could be ester bound either to another FA (predominantly linoleic acid (C18:2)) (EO) or to glutamate residues of the proteins (mostly involucrin) at the surface of a corneocyte (PO). The letter **E** precedes for ceramide esterified with another FA, and **P** for ceramides bound to proteins. In addition, Rabionet et al. [29] have identified the class of 1-O-acylceramides (1-O-AcylCers) with three hydrophobic chains, the third chain ester-linked to the primary hydroxyl in position 1 of the sphingoid base (1-O-E), as 1-O-ENS and 1-O-EAS ceramides. Noteworthy, this complexity can be encountered also in ceramide precursors: glucosylceramides and sphingomyelins classes, contributing to complex molecular heterogeneity of epidermal lipids.

Lipid epidermis profiling and molecular characterization represents a real analytical challenge and requires the use of a highly efficient chromatographic separation coupled to mass spectrometric detection.

In RP-LC, the retention of lipid molecular species is mainly governed by the extent of interaction between the hydrocarbonaceous moiety of the molecule and the stationary phase where the nature of the polar group is playing a minor role [30]. NPLC remains interesting to the analysis of a total lipid extract and the objective to a complete separation of lipid classes [15, 31–35]. The mobile phases are usually made of solvent mixtures to ensure miscibility and to encompass a wide range of polarity. The main advantage of NPLC is the elution of lipids according to their polar moieties or "head group" which also defines their family or "lipid class." In complex lipid mixtures analysis, NPLC produces easily interpreted chromatograms in which molecular species of the same class co-elute within a single peak. Mass spectrometry is

normally used to access the molecular species identification and relative distribution [32].

In this configuration, the selection of the most appropriate interface with the mass spectrometry represents an important element in the development of the analytical method, because the ionization mode could have a significant impact on the detection of molecules. According to the literature, ESI does not allow the detection of the whole lipid classes especially the non-polar lipids [30, 32, 36]. In addition, important ceramides with a ω-ester linkage, such as Cer [EOS], Cer [EOP], and Cer [EOH], were not accessible [13]. Coupled with APCI, provided satisfactory results, but APPI is generally more sensitive and does not require any dopant make-up in NPLC chromatographic conditions [32].

In this publication, we suggest an analytical method for the structural identification and the overall evaluation of all molecules in epidermis lipid classes and subclasses (cited above). The developed approach has been used to characterize the lipids of reconstructed human epidermis especially the biomarkers of the keratinocyte differentiation. In addition, we describe a new class of epidermal ceramides. These ceramides contain an ultra-long chain esterified with a linoleic acid in the N- position and a long to very long acyl chains in the 1-O-position of the sphingoid base. We suggest naming these compounds 1-O-E (EO) Cer. Considering their chemical structure and hydrophobicity, we expect that this new identified subclass contributes to the skin barrier. Moreover, up until now, sphingomyelins were considered precursors exclusively for sphingosine-containing NS- and AS-ceramides. In this work, we characterized several sphingomyelin subclasses which could be precursors of other ceramide subclasses such as NdS, NP, NH, NT, AH, AdS, AP, EOS, and EOH. This new chemical information leads to biological interpretations that could be very interesting in understanding the barrier function.

Material and method

Chemicals

All analytical standards (tripalmitin (TG (16:0/16:0/16:0)), dipalmitin (DG (16:0/16:0)), monostearin (MG (18:0)), cholesterol (Chol), palmitic acid (FFA (16:0)), ceramide 1 (EOS (d18:1/26:0/18:1)), ceramide 9 (EOP (t18:0/26:0/18:1)), ceramide 3 (NP (t18:0/18:0)), ceramide 3A (NP (t18:0/18:2)), ceramide 3B (NP (t18:0/18:1)), and ceramide 6 (AP (t18:0/18:0))); glucosylceramides (GlcCER); phospholipids (PL) (phosphatidylinositol (PI), phosphatidylcholine (PC), phosphatidylethanolamine (PE)); and sphingomyelins (SM)) were purchased from Sigma-Aldrich (Saint Quentin Fallavier, France).

Glucosylceramides (GlcCER (d18:2/16:0)) and sphingomyelins (SM (d18:1/12:0)) mono-compounds were purchased from Avanti Polar Lipids, Inc. (Alabaster, AL, USA) for fragmentation investigative.

Solvents for extraction and for NPLC/APPI-HR-MS^n were of HPLC grade and were all purchased from Sigma-Aldrich (Saint Quentin Fallavier, France).

Lipid mixture

Test mixture is composed by 14 lipids standards: tripalmitin (TG), dipalmitine (DG), cholesterol (Chol), palmitic acid (FFA), monostearin (MG), ceramide 1 EOS, ceramide 9 EOP, ceramide 3 NP, ceramide 6 AP, glucosylceramides (GlcCER), phospholipids (PL) (phosphatidylinositol (PI), phosphatidylcholine (PC), phosphatidylethanolamine (PE)) and sphingomyelins (SM), at an individual concentration of 0.5 g/L in chloroform.

Instrumentation and analytical method NPLC/APPI-MS

Samples were analyzed in HPLC (Dionex Ultimate 3000, ThermoFisher Scientific, San Jose, CA). The separation of the lipids was carried out in normal-phase liquid chromatography using a polyvinyl alcohol (PVA)-Sil column (PVA-bonded column; 5 μm particle size, 150 × 4.6 mm) purchased from YMC (Kyoto, Japan). NPLC was performed using a solvent gradient of heptane/ethyl acetate (99.8:0.2 v/v) (Solvent A), acetone and ethyl acetate (2:1 v/v) with acetic acid (0.02% v/v) (solvent B), and 2-propanol/water (85:15, v/v) (with acetic acid and ethanolamine each at 0.025% v/v) (solvent C). The mobile phases and the solvent program are presented in Table 1. The flow rate was set at 1 mL min^{-1}. The injected volume was 10 μL.

The outgoing LC flow rate was split in post-column into two detectors: a Corona CAD® and an hybrid mass spectrometer LTQ-Orbitrap Velos Pro (Thermo Fisher Scientific, San Jose, CA) equipped with an atmospheric pressure photoionization (APPI). A negative APPI was used for analysis of free fatty acids and a positive APPI for the identification of the other lipid classes. The APPI heater was set to 400 °C and the heated capillary to 350 °C. Sheath gas and auxiliary gas flow rates were set at 40 and 5 L/min respectively. The mass scan range was 220–1800 atomic mass units (amu). A full scan detection mode and fragmentation was performed by the orbital trap at a resolution of 100,000. The MS^2/MS^3 spectra were obtained simultaneously in data-dependent acquisition (DDA) mode. Fragmentation was performed in CID (collision-induced dissociation) at 35 eV of collision energy in positive ionization mode in the double linear trap with high resolution. For MS^2, CID was performed on the 5 most abundant precursor ions with a signal threshold 10^{+3}. For MS^3, CID was performed on the 3 most abundant ions with a signal threshold 10^{+3}. Dynamic exclusion parameters were

Table 1 Composition of the ternary gradient of the mobile phase in NPLC/HR-MS^n. Phase A: heptane/ethyl acetate (99.8:0.2, v/v), B: acetone/ethyl acetate (2:1 v/v) with acetic acid (0.02% v/v), and C: 2-propanol/water (85:15, v/v) (with acetic acid and ethanolamine each at 0.025% v/v)

Temps (min)	Phase A (%)	Phase B (%)	Phase C (%)
0	100	0	0
3	100	0	0
5	97	3	0
10	94	6	0
15	80	20	0
20	70	30	0
25	60	40	0
30	50	50	0
35	46	39	15
40	40	30	30
50	40	0	60
51	40	0	60
56	0	100	0
61	0	100	0
62	100	0	0
74	100	0	0

as follows: repeat count, 3 of each parent ion; repeat duration, 30 s; exclusion duration, 15 s; and exclusion mass, 1.5 uma. Analyses were performed using Thermo Fisher Xcalibur software. Data were searched at ± 10 ppm between theoretical mass experimental values.

Artificial skin

Episkin® (Episkin, France) is a reconstructed human epidermis (RHE) model obtained from the culture of normal human-derived epidermal keratinocytes (NHEK) on polycarbonate filters in the interface air-liquid. Culture diameter is 0.5 cm^2 for each sample. Over 11 days of culture, RHE represents a multilayered model of the human epidermis. Samples were received at age of 11 days, then transferred into the medium supplied by the provider and incubated until D22 in CO_2 at 37 °C.

Extraction procedure

Total lipids of cell cultures were extracted by the modified methods of Folch [37, 38] and Bligh and Dyer [39]. The epidermis was separated from the polycarbonate filters using pliers, placed into 1.5 mL of methanol, then vortexed for 2 min. Three milliliters of chloroform was added and the agitation of the whole volume was done at room temperature during 1 h in the dark. For the separation phase, 1.5 mL of water was added and mixed using a magnetic agitator for

10 min at room temperature. Centrifugation at 3000 rpm for 10 min at 20 °C was done. Recovery for the organic phase was achieved. Two milliliters of chloroform was added on the aqueous phase (H_2O + methanol + skin) as a washing phase and the whole mixture was vortexed and centrifuged for 10 min at 3000 rpm and at 20 °C. The organic phase was collected and evaporated under a stream of nitrogen until dryness. The lipid residue was taken up with 20 μL of chloroform.

Results

Chromatographic separation

Our objective was to achieve the highest degree of separation allowing the characterization of epidermis lipidome. For this purpose, a developed analytical method was tested on a mixture composed of 14 lipid standards representing all lipid classes in the epidermis. Separation of lipids was based on the NPLC method developed by Graeve et al. [15]. The elution gradient was the increasing polarity to increase eluting force. The initial eluent n-heptane modified with 0.2% ethyl acetate (solvent A) was selected because of its low polarity to separate non-polar lipids. Separation of triglycerides, diglycerides, and monoglycerides was achieved with a slow increase of solvent B from 3 to 6% during 5.0 min after the initial period of 5 min of the gradient program. The final proportion of 50% solvent B was found to be optimal for the separation of the remaining neutral lipids such as free fatty acids and especially ceramide subclasses. All neutral lipids were fully eluted before 38 min. With increasing proportions of eluent C, the polar lipids were eluted such as phospholipids and sphingomyelins (Table 2). As a final step, a progressive return to initial conditions was achieved, using first solvent B (5 min) followed by solvent A

Table 2 Retention time of analytical standards lipids in NPLC/HR-MS^n

Analytical standards	Retention time (min)
Tripalmitin (TG)	10.36
Dipalmitin (DG)	14.59
Cholesterol (Chol)	15.12
Palmitic acid (FFA)	15.6
Monostearin (MG)	20.43
Ceramide 1 EOS	21.11
Ceramide 9 EOP	21.75
Ceramide 3 NP	23.74
Ceramide 6 AP	24.84 and 27.91
Glucosylceramides (GlcCER)	36.96
Phospholipids (PL: PI, PC, PE)	40–43
Sphingomyelins (SM)	44.16

(12 min) at 1 mL/min. The total run time between injections and elution of all lipid classes was 51 min.

Therefore, we optimized new analytical conditions allowing a good separation of the overall lipid classes. Moreover, an ideal elution window of the ceramide subclasses in the area of medium polarity lipids with retention times intermediate between monoglycerides (MG) and glucosylceramides (GlcCER) was obtained. In addition, this gradient profile offers the possibility to separate sphingomyelins from the other phospholipids which represent a close degree of polarity. In summary, we were able in a single run to analyze all epidermis lipids with a good resolution, and especially, to separate the 3 classes (and subclasses) of interest for our biological objective: ceramides, glucosylceramides, and sphingomyelins (Fig. 1).

Identification of MS fragments

The study of fragmentation was carried out on analytical standards representing the overall epidermis lipid classes. In full scan mass spectra, one or two major ions of each lipid have been identified: $[M-H]^-$ for free fatty acid, $[M+H-FA]^+$ for triglycerides, $[M+H-H_2O]^+$ for monoglycerides, diglycerides, and cholesterol. Regarding phospholipids class, we observed systematically $[M+H-polar\ head]^+$ while $[M+H]^+$ or $[M+Na]^+$ were detected depending on phospholipids type (PI, PC, or PE).

For non-esterified ceramides (such as NP, AP), two groups of interest were obtained in full scan and MS^2: on the first hand, the molecular peak and the losses of several water molecules corresponding to the total number of hydroxyl groups on the ceramide polar head, on the other hand, the fragments of the sphingoid base part and the fatty acid part.

However, for esterified ceramides (such as EOS, EOP), a third additional group is obtained which gives information on the acid part combined to the ester moiety or the acid part combined to the base without the ester moiety (Fig. 2).

Regarding glucosylceramide and sphingomyelin, they were fragmented in the ionization source. Thus, we collected all information from the full scan mass spectra.
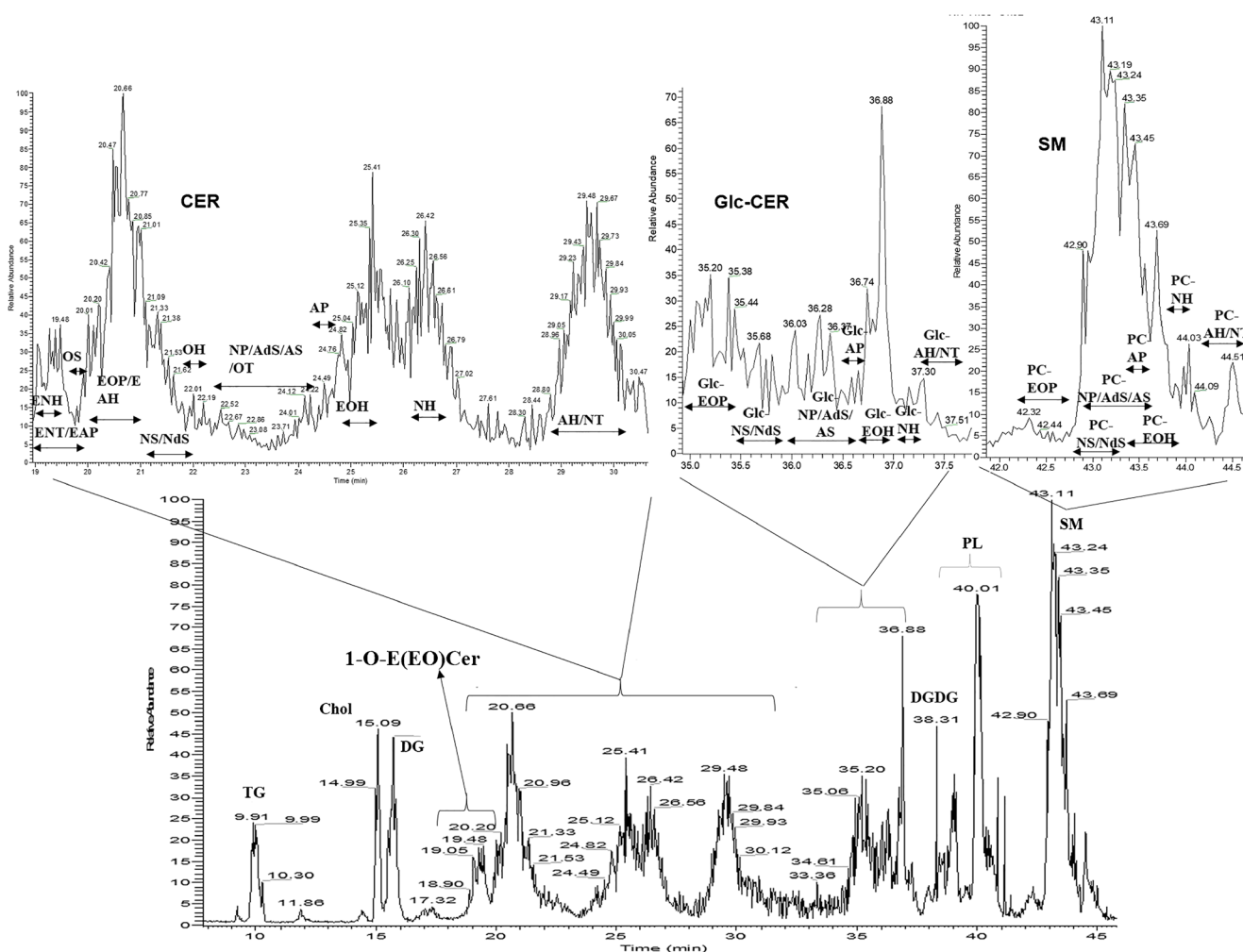

Fig. 1 NPLC/Corona® chromatographic profile of lipid classes and subclasses obtained for the RHE culture at D22
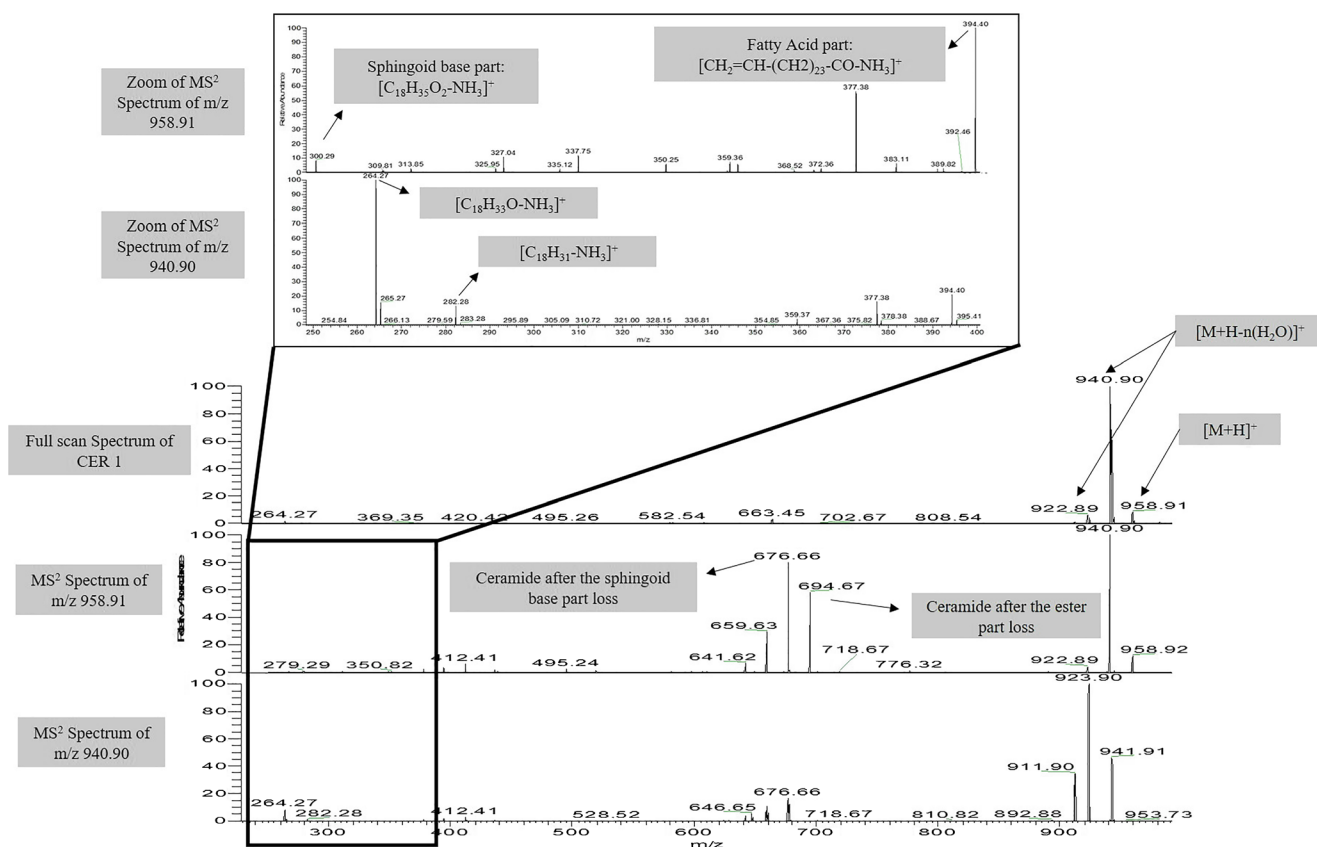
Fig. 2 Mass spectra obtained in full scan and MS^2 of esterified ceramide: ceramide 1 (EOS, $C_{62}H_{119}NO_5$ (d18:1/26:0/18:1))

Non-esterified ceramides

Ceramides 3 (NP, $C_{36}H_{73}NO_4$, t18:0/18:0), 3A (NP, $C_{36}H_{69}NO_4$, t18:0/18:2), and 3B (NP, $C_{36}H_{71}NO_4$, t18:0/18:1) The ceramide 3 carries 3 hydroxyls on its base moiety. In full scan mass spectrum, we detected the molecular peak $[M+H]^+$ at m/z 584.56 and the losses of three water molecules corresponding to m/z 566.55, 548.54, and 530.53.

Fragmentation was achieved for the two most intense peaks of m/z 584.56 and 566.55.

Fragments exposed below could be obtained from the fragmentation of m/z 584.56 and/or m/z 566.55 using MS^2 mode.

Thus, we observed the peak of the sphingoid base part $[CH_3\text{-}(CH_2)_{13}\text{-}(CH(OH))_2\text{-}CH(CH_2OH)\text{-}NH_3]^+$ at m/z 318.29 $[C_{18}H_{40}NO_3]^+$ and fragments corresponding to three water losses at m/z 300.29 $[C_{18}H_{38}NO_2]^+$, 282.28 $[C_{18}H_{36}NO]^+$, and 264.27 $[C_{18}H_{34}N]^+$.

In addition, the fragment $[CH_3\text{-}(CH_2)_{16}\text{-}CO\text{-}NH_3]^+$ m/z 300.29 $[C_{18}H_{38}NO]^+$ corresponds to the fatty acid part $[FA+ NH_3]^+$.

For ceramides 3A and 3B, the fragmentation is the same as ceramide 3 but with one unsaturation on the fatty acid part of CER 3B and two unsaturations on the fatty acid part of CER 3A. Then, in MS^2 spectra, the fatty acid part of CER 3B and CER 3A was observed at m/z 280.26 $[C_{18}H_{34}NO]^+$ and m/z 282.28 $[C_{18}H_{36}NO]^+$ respectively (Fig. 3c).

Thus, in the case of CER 3A, $[C_{18}H_{36}NO]^+$ is obtained from two fragmentation ways, one from the sphingoid base part and the second from the fatty acid part.

The characteristic fragments of the acid part as well as the base part are very useful in the determination of the carbon chain length and especially the number of unsaturation and hydroxyl groups that could be carried by each chain. This information reinforces the hypothesis on the corresponding ceramide subclass.

Ceramide 6 (AP, $C_{36}H_{73}NO_5$, (t18:0/18:0)) This ceramide contains 4 hydroxyl groups on its polar head of which one is on the fatty acid part. Similarly, in full scan spectrum, we observed the molecular peak $[M+H]^+$ at m/z 600.55 with the losses of four water molecules at m/z 582.54, 564.53, 546.52, and 528.51.

Fragments exposed below could be obtained from the fragmentation of m/z 600.55 and/or m/z 582.54 using MS^2 mode.

Thus, we observed the peak of the sphingoid base part $[CH_3\text{-}(CH_2)_{13}\text{-}(CH(OH))_2\text{-}CH(CH_2OH)\text{-}NH_3]^+$ at m/z 318.29 $[C_{18}H_{40}NO_3]^+$ and fragments corresponding to three
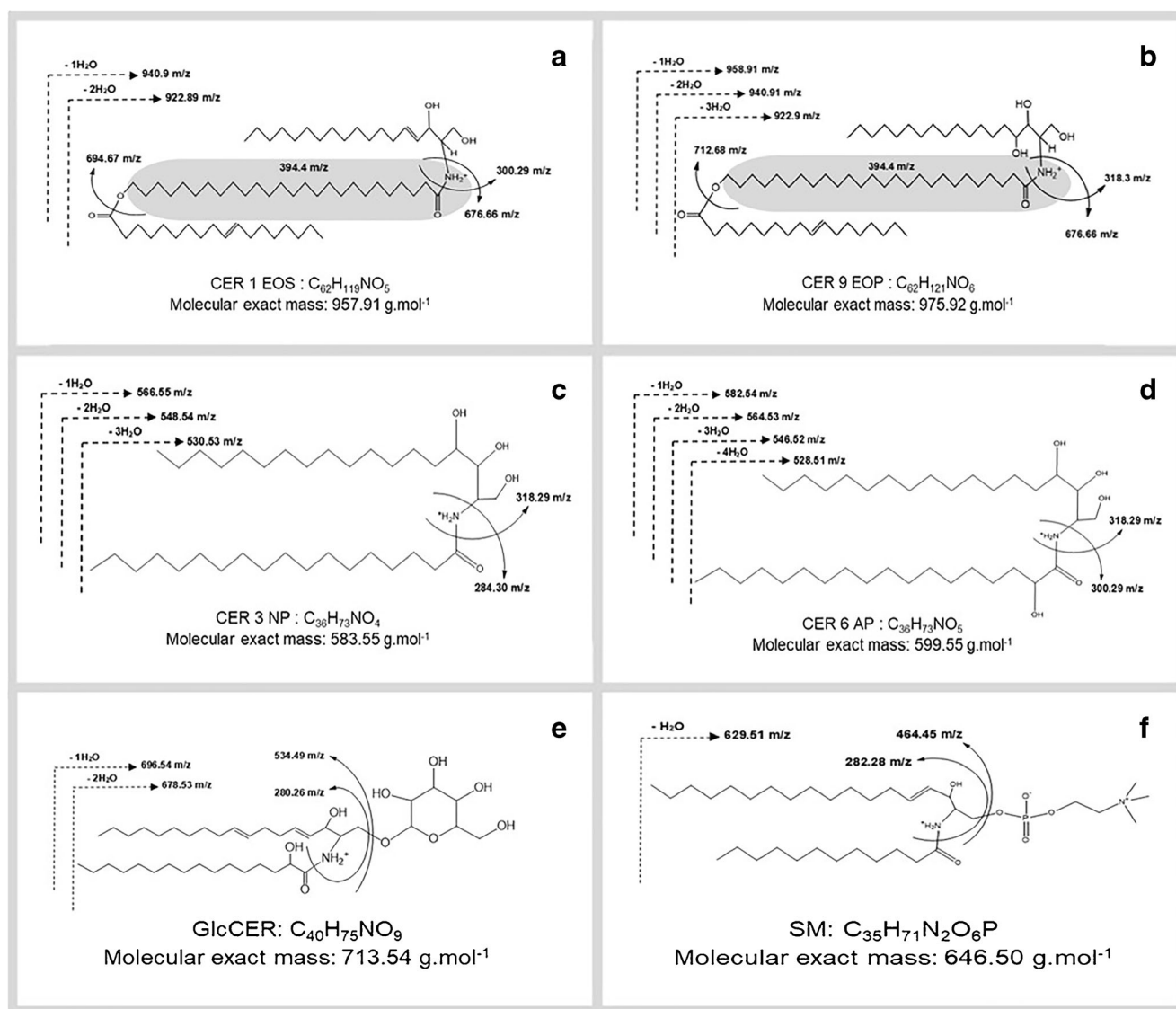
Fig. 3 The characteristic fragments observed in full scan and MS^2 spectra of analytical standards of ceramides: **a** CER 1 EOS, **b** CER 9 EOP, **c** CER 3 NP, **d** CER 6 AP, **e** GlcCER, **f** SM

water losses at m/z 300.29 $[C_{18}H_{38}NO_2]^+$, 282.28 $[C_{18}H_{36}NO]^+$, and 264.27 $[C_{18}H_{34}N]^+$.

In addition, the fragment $[CH_3\text{-}(CH_2)_{15}\text{-}CH(OH)\text{-}CO\text{-}NH_3]^+$ m/z 300.29 $[C_{18}H_{38}NO_2]^+$ corresponds to the fatty acid part $[FA+NH_3]^+$ (Fig. 3d).

Thus, $[C_{18}H_{38}NO_2]^+$ is obtained from two fragmentation ways, one from the sphingoid base part and the second from the fatty acid part.

Esterified ceramides

Ceramide 1 (EOS, $C_{62}H_{119}NO_5$ (d18:1/26:0/18:1)) This ceramide is esterified on the ω position of its acid part and contains 2 hydroxyl groups on its base part moiety.

In the full scan spectrum, we observed the molecular peak $[M+H]^+$ m/z 958.92 with two water losses of m/z 940.9 and m/z 922.89 corresponding to the number of hydroxyl groups.

Fragments exposed below could be obtained from the fragmentation of m/z 958.91 and/or m/z 940.9 using MS^2 mode.

Therefore, we observed m/z 300.29 corresponding to the sphingoid base part $[C_{18}H_{35}O_2\text{-}NH_3]^+$ with fragments resulting from the losses of two water molecules at m/z 282.28 and m/z 264.27. In addition, we detected m/z 676.66 related to the acid part with the ester $[CH_3\text{-}(CH_2)_6\text{-}CH=CH\text{-}(CH_2)_8\text{-}COO\text{-}(CH_2)_{25}\text{-}CO\text{-}NH_3]^+$; the m/z 394.4 corresponding to the fatty acid part $[FA+NH_3]^+$ only without the ester part $[CH_2=CH\text{-}(CH_2)_{23}\text{-}CO\text{-}NH_3]^+$ was observed. Finally, the m/z 694.67 corresponds to the ceramide after the loss of the ester of the fatty acid part $[CH_3\text{-}(CH_2)_{12}\text{-}CH=CH\text{-}$

CH(OH)-CH(CH$_2$OH)-NH-CO-(CH$_2$)$_{24}$-CH$_2$-OH,H]$^+$ (Figs. 2 and 3a).

Ceramide 9 (EOP, C$_{62}$H$_{121}$NO$_6$, (t18:0/26:0/18:1)) This ceramide is esterified on the ω position of its fatty acid part and contains 3 hydroxyl groups on its sphingoid base part.

In the full scan spectrum, we observe the molecular peak [M+H]$^+$ at *m/z* 976.92 with the losses of three water molecules at *m/z* 958.91, 940.91, and 922.9.

The fragmentation of *m/z* 976.92 and/or *m/z* 958.91 using MS^2 mode allowed the detection of: *m/z* 318.3 corresponding to the sphingoid base part [C$_{18}$H$_{37}$O$_3$-NH$_3$]$^+$ and all the losses of three water molecules at *m/z* 300.29, 282.28, and 264.27. Moreover, *m/z* 676.66 corresponding to the acid part with the ester [CH$_3$-(CH$_2$)$_6$-CH=CH-(CH$_2$)$_8$-COO-(CH$_2$)$_{25}$-CO-NH$_3$]$^+$ and the *m/z* 394.4 matching the fatty acid part [FA+NH$_3$]$^+$ only without the ester part [CH$_2$=CH-(CH$_2$)$_{23}$-CO-NH$_3$]$^+$ were evidenced. Finally, the *m/z* 712.68 related to the ceramide after the loss of the ester of the fatty acid part [CH$_3$-(CH$_2$)$_{13}$-CH(OH)-CH(OH)-CH(CH$_2$OH)-NH-CO-(CH$_2$)$_{24}$-CH$_2$-OH,H]$^+$ was observed (Fig. 3b).

Glucosylceramide (C40H75NO9, (d18:2/16:0))

In the full scan mass spectrum, we observed the molecular peak [M+H]$^+$ at *m/z* 714.55 which was associated with the fragment representing water molecule losses at *m/z* 696.54 and 678.53 that correspond to the hydroxyl groups carried by the fatty acid moiety and the base moiety.

However, glucosylceramide has lost the glucose moiety in the ionization source; thus, we detected [M+H-180]$^+$ at *m/z* 534.49, which was associated with *m/z* 516.48 and 498.47 due to the losses of two water molecules.

Finally, we observed *m/z* 280.26 matching the sphingoid base part after fatty acid part cleavage [CH$_3$-(CH$_2$)$_8$-CH=CH-(CH$_2$)$_2$-CH=CH-CH(OH)-C(CH$_2$)-NH$_3$]$^+$ and one water molecule loss at *m/z* 262.25 (Fig. 3e).

Sphingomyelin (C$_{35}$H$_{71}$N$_2$O$_6$P, (d18:1/12:0)

Similarly, the sphingomyelin was fragmented in the ionization source. Then, in the full scan spectrum, we observed the molecular peak [M+H]$^+$ *m/z* 647.51 with one water molecule loss at *m/z* 629.51 corresponding to the hydroxyl group carried by the base moiety.

However, sphingomyelin has mainly lost the phosphocholine group in the ionization source; thus, we detected [M+H-183]$^+$ at *m/z* 464.45, which was more intense than the molecular peak, and we observed one water molecular loss at *m/z* 446.44.

Finally, we characterized the fragment corresponding to the sphingoid base part after the fatty acid part cleavage [CH$_3$-(CH$_2$)$_{12}$-CH=CH-CH(OH)-C(CH$_2$)-NH$_3$]$^+$ at *m/z* 282.28 and one water molecule loss at *m/z* 264.27 (Fig. 3f).

Characterization of lipid epidermis

After the development of the separation protocol and the characterization method of ceramides as well as glucosylceramides and sphingomyelins, this method was used to study a biological sample: the reconstructed human epidermis at the 22nd day (D22) of differentiation. The lipids were extracted and analyzed using our approach, in which the totality of different lipid classes was detected: triglycerides, cholesterols, diglycerides, free fatty acids, and ceramides were eluted between 20 and 30 min, glucosylceramides detected at 36 min, and finally phospholipids and sphingomyelins detected at 40 and 43 min respectively (Fig. 1). The identification of ceramide subclasses, as well as glucosylceramides and sphingomyelins, was then achieved based on characteristic fragments defined above. For example, the most intense ceramide molecules in each class are exposed in Table 3. Thus, 15 subclasses of ceramides were determined. Based on a sphingoid base, we resume the identified ceramides and we indicate the range of the total carbon number of each subclass: sphingosine S: NS (C41–C48), AS (C34–C56), OS (C52–C56), EOS (C64–C72); dihydrosphingosine dS: NdS (C41–C48), Ads (C34–C56); phytosphingosine P: NP (C34–C56), AP (C42–C52), EAP (C58–60); 6-hydroxysphingosine H: NH (C33–C48), AH (C44–C54), OH (C50–57), ENH (C61–66), EAH (C58–C64), EOH (C64-C70); and tetrahydroxylated sphingoid base T: NT (C44–C54), OT (C50–56), ENT (C57–60) (Tables 4 and 5). In all subclasses, ceramides were saturated or unsaturated with one or two degrees of unsaturation on fatty acid moiety, and double unsaturation for ester chain when the ceramides are linked to linoleic acid.

In addition, we identified the glucosylceramides and sphingomyelins.

Interestingly, comparing the molecular composition of ceramides, glucosylceramides, and sphingomyelins, we are seeing the complete similitude of the ceramide moieties overall of these three lipid classes in terms of the total numbers of carbons, unsaturation, and hydroxyl groups on the polar head. Table 3 summarizes all identified classes and subclasses.

Identification of a novel ceramide subclass

A new ceramide subclass was detected in RHE sample; it was eluted at retention time between 19.0 and 20.0 min (Table 6). The particularity of this subclass is that the ceramide is double esterified: on the 1-O-position of sphingoid base with a long to very long chain acyl residues

Table 3 The identified ceramides, glucosylceramides, and sphingomyelins in a biological sample (RHE at D22). The first 3 columns show the identified subclasses of ceramides then their molecular formula and their retention time in columns 4 and 5 respectively. Columns 6 and 7 represent respectively the molecular formula and the retention time of identified glucosylceramides (if present) for each ceramide subclass. Finally, columns 8 and 9 show respectively the molecular formula and the retention time of identified sphingomyelins (if present) for each ceramide subclass. Different molecules could be co-eluted at the same retention time

Identified ceramide subclasses		Ceramides		Glucosylceramides		Sphingomyelins	
		Molecular formula	RT (min)	Molecular formula	RT (min)	Molecular formula	RT (min)
E(18:0) N(28:0) H(20:1)		$C_{66}H_{129}NO_5$	19.32				
E(18:0) N(26:0) H(20:1)		$C_{64}H_{125}NO_5$	19.39				
E(18:0) N(26:0) H(18:1)		$C_{62}H_{121}NO_5$	19.46				
E(18:0) N(27:0) H(18:1)		$C_{63}H_{123}NO_5$	19.48				
E(18:0) N(24:0) T(18:0)		$C_{60}H_{119}NO_6$	19.53				
E(18:0) A(24:0) P(18:0)							
E(18:0) N(25:0) H(18:1)		$C_{61}H_{119}NO_5$	19.54				
E(18:0) N(23:0) T(18:0)		$C_{59}H_{117}NO_6$	19.68				
E(18:0) A(24:0) P(17:0)							
E(18:0) N(22:0) T(18:0)		$C_{58}H_{115}NO_6$	19.75				
E(18:0) A(24:0) P(16:0)							
E(18:0) N(22:0) T(17:0)		$C_{57}H_{113}NO_6$	19.84				
E(18:2) O(30:1) S(18:0)	E(18:2) O(28:1) S(20:0)	$C_{66}H_{127}NO_5$	19.99	$C_{72}H_{137}NO_{10}$	35.29		
E(18:2) O(28:2) S(18:1)	E(18:2) O(26:2) S(20:0)	$C_{64}H_{123}NO_5$	20.06				
E(18:2) A(24:0) H(18:1)		$C_{60}H_{117}NO_6$	20.26				
E(18:2) A(24:0) H(16:1)		$C_{58}H_{113}NO_6$	20.5				
E(18:2) O(32:2) S(22:0)		$C_{72}H_{137}NO_5$	20.62	$C_{78}H_{147}NO_{10}$	36.03	$C_{77}H_{149}N_2PO_8$	41.82
E(18:2) O(31:2) S(22:0)		$C_{71}H_{135}NO_5$	20.74	$C_{77}H_{145}NO_{10}$	35.88	$C_{76}H_{147}N_2PO_8$	41.96
E(18:2) O(30:2) S(20:0)		$C_{68}H_{129}NO_5$	20.9	$C_{74}H_{139}NO_{10}$	35.29	$C_{73}H_{141}N_2PO_8$	41.82
N(30:0) S(18:1) / N(29:1) dS(19:0)	N(26:0) S(22:0) / N(26:1) dS(22:0)	$C_{48}H_{95}NO_3$	21.15	$C_{54}H_{105}NO_8$	35.88	$C_{53}H_{107}N_2PO_6$	42.62
N(28:0) S(18:1) / N(28:1) dS(18:0)	N(24:0) S(22:0) / N(27:1) dS(19:0)	$C_{46}H_{91}NO_3$	21.28	$C_{52}H_{101}NO_8$	36.18	$C_{51}H_{103}N_2PO_6$	42.81
N(28:0) S(19:1) / N(28:1) dS(19:0)	N(26:0) S(21:0) / N(26:1) dS(21:0)	$C_{47}H_{93}NO_3$	21.3	$C_{53}H_{103}NO_8$	35.96	Not found	
N(26:0) S(18:1) / N(27:1) dS(17:0)	N(23:1) dS(21:0)	$C_{44}H_{87}NO_3$	21.36	$C_{50}H_{97}NO_8$	36.18	$C_{49}H_{99}N_2PO_6$	43
N(27:0) S(18:1) / N(27:1) dS(18:0)	N(25:0) S(20:0) / N(24:1) dS(21:0)	$C_{45}H_{89}NO_3$	21.37	$C_{51}H_{99}NO_8$	36.18	$C_{50}H_{101}N_2PO_6$	42.55
N(25:0) S(18:1) / N(25:1) dS(18:0)	N(23:0) S(20:0) / N(23:1) dS(20:0)	$C_{43}H_{85}NO_3$	21.52	$C_{49}H_{95}NO_8$	36.33	$C_{48}H_{97}N_2PO_6$	43.06
N(26:0) S(16:1) / N(26:1) dS(16:0)	N(22:0) S(20:0) / N(23:1) dS(19:0); N(24:0) S(18:0) / N(24:1) dS(18:0)	$C_{42}H_{83}NO_3$	21.59	$C_{48}H_{93}NO_8$	36.4	$C_{47}H_{95}N_2PO_6$	43.19

Table 3 (continued)

Identified ceramide subclasses		Ceramides		Glucosylceramides		Sphingomyelins	
		Molecular formula	RT (min)	Molecular formula	RT (min)	Molecular formula	RT (min)
N(24:0) S(17:0) N(24:1) dS(17:0)	N(25:0) S(16:1) N(25:1) dS(16:0)	$C_{41}H_{81}NO_3$	21.66	$C_{47}H_{91}NO_8$	36.55	$C_{46}H_{93}N_2PO_6$	43.3
N(18:0) P(18:0) A(18:0) dS(18:0)	N(20:0) P(16:0) A(20:0) dS(16:0)	$C_{36}H_{73}NO_4$	22.12	$C_{42}H_{83}NO_9$	37.07	$C_{41}H_{85}N_2PO_7$	43.93
N(17:0) P(17:0) A(17:0) dS(17:0)	N(18:0) P(16:0) A(18:0) dS(16:0)	$C_{34}H_{69}NO_4$	22.26	$C_{40}H_{79}NO_9$	37.14	$C_{39}H_{81}N_2PO_7$	42.81
N(24:0) P(24:0) A(27:0) dS(21:0)	N(26:0) P(22:0) A(28:0) dS(20:0)	$C_{48}H_{97}NO_4$	22.78	$C_{54}H_{107}NO_9$	36.55	$C_{53}H_{109}N_2PO_7$	42.62
N(28:0) P(18:0) A(27:0) dS(19:0)	N(24:0) P(22:0) A(28:0) dS(18:0)	$C_{46}H_{93}NO_4$	22.98	$C_{52}H_{103}NO_9$	36.93	Not found	
N(24:0) P(20:0) A(25:0) dS(19:0)	N(26:0) P(18:0) A(26:0) dS(18:0)	$C_{44}H_{89}NO_4$	22.99	$C_{50}H_{99}NO_9$	36.93	$C_{49}H_{101}N_2PO_7$	43.3
N(26:0) P(16:0) A(24:0) dS(18:0)	N(24:0) P(18:0) A(26:0) dS(16:0)	$C_{42}H_{85}NO_4$	23.14	$C_{48}H_{95}NO_9$	37	$C_{47}H_{97}N_2PO_7$	43.49
N(26:0) P(17:0) A(17:0) dS(26:0)	N(25:0) P(18:0) A(18:0) dS(25:0)	$C_{43}H_{87}NO_4$	23.2	$C_{49}H_{97}NO_9$	36.63	$C_{48}H_{99}N_2PO_7$	43.36
N(23:0) P(18:0) A(22:0) dS(18:0)	N(24:0) P(17:0) A(23:0) dS(16:0)	$C_{41}H_{83}NO_4$	23.44	$C_{47}H_{93}NO_9$	36.93	$C_{46}H_{95}N_2PO_7$	43.56
N(23:0) P(17:0)	N(24:0) P(16:0)	$C_{40}H_{81}NO_4$	23.57	$C_{46}H_{91}NO_9$	37.07	$C_{45}H_{93}N_2PO_7$	43.72
N(32:2) P(24:0) A(32:1) S(24:0) A(34:2) dS(22:0)	N(34:2) P(22:0) A(34:1) S(22:1) A(35:2) dS(21:0)	$C_{56}H_{109}NO_4$	23.95	$C_{62}H_{119}NO_9$	36.82	Not found	
N(32:1) P(22:0) A(32:0) S(22:1)	N(30:1) P(22:0) A(30:0) S(22:1)	$C_{52}H_{103}NO_4$	24.19	$C_{58}H_{113}NO_9$	36.88	$C_{57}H_{115}N_2PO_7$	42.55
N(32:2) P(20:0) A(32:1) S(20:0) A(34:2) dS(21:0)	N(34:2) P(18:0) A(34:1) S(18:1) A(31:2) dS(21:0)	$C_{52}H_{101}NO_4$	24.34	$C_{58}H_{111}NO_9$	36.88	$C_{57}H_{113}N_2PO_7$	43.56
N(30:1) P(20:0) A(30:0) S(20:0)	N(32:1) P(18:0) A(32:0) S(18:1)	$C_{50}H_{99}NO_4$	24.42	$C_{56}H_{109}NO_9$	36.93	$C_{55}H_{111}N_2PO_7$	43.64
N(34:2) P(22:0) A(32:1) S(22:0)	N(34:2) P(20:0) A(34:1) S(20:1) A(35:1) dS(19:0)	$C_{54}H_{105}NO_4$	24.43	$C_{60}H_{115}NO_9$	36.88	Not found	
N(28:1) P(22:0) A(26:0) S(20:0)	N(30:1) P(18:0) A(30:0) S(18:1) A(31:1) dS(17:0)	$C_{48}H_{95}NO_4$	24.51	$C_{54}H_{105}NO_9$	36.93	$C_{53}H_{107}N_2PO_7$	43.85
N(30:2) P(20:0) A(30:1) S(20:0)	N(32:2) P(18:0) A(32:1) S(18:1)	$C_{50}H_{97}NO_4$	24.6	$C_{56}H_{107}NO_9$	36.93	$C_{55}H_{109}N_2PO_7$	43.72

Table 3 (continued)

Identified ceramide subclasses			Ceramides		Glucosylceramides		Sphingomyelins	
			Molecular formula	RT (min)	Molecular formula	RT (min)	Molecular formula	RT (min)
A(32:2) dS(19:0)	A(31:2) dS(19:0)	A(29:2) dS(21:0)						
A(32:1) P(18:0)	A(30:1) P(20:0)	A(28:1) P(22:0)	$C_{50}H_{99}NO_5$	24.6	$C_{56}H_{109}NO_{10}$	37.14	$C_{55}H_{111}N_2PO_8$	43.93
A(34:1) P(18:0)	A(32:1) P(20:0)	A(30:1) P(22:0)	$C_{52}H_{103}NO_5$	24.68	$C_{58}H_{113}NO_{10}$	37.22	$C_{57}H_{115}N_2PO_8$	43.79
N(30:1) P (17:0); A(30:0) S (17:1); A(30:1) dS(17:0)	N(29:1) P(18:0); A(29:0) S(18:0); A(29:1) dS(18:0)	N(26:1) P(21:0); A(26:0) S(21:0); A(26:1) dS(21:0)	$C_{47}H_{93}NO_4$	24.9	$C_{53}H_{103}NO_9$	36.93	$C_{52}H_{105}N_2PO_7$	43.93
N(27:1) P(18:0); A(27:0) S(18:1); A(27:1) dS(18:0)	N(25:1) P(20:0); A(25:0) S(20:0); A(25:1) dS(20:0)	N(24:1) P(21:0); A(24:0) S(21:0); A(24:1) dS(21:0)	$C_{45}H_{89}NO_4$	24.96	$C_{51}H_{99}NO_9$	36.93	$C_{50}H_{101}N_2PO_7$	43.19
N(28:1) P(18:0); A(28:0) S(18:1); A(28:1) dS(18:0)	N(26:1) P(20:0); A(26:0) S(20:0); A(24:1) dS(21:0)	N(24:1) P(22:0); A(24:0) S(22:0)	$C_{46}H_{91}NO_4$	25.1	$C_{52}H_{101}NO_9$	36.93	$C_{51}H_{103}N_2PO_7$	43.06
N(25:1) P(17:0); A(25:0) S(17:1); A(25:1) dS(16:0)	N(24:1) P(18:0); A(24:0) S(18:0); A(24:1) dS(17:0)	N(20:1) P(22:0); A(20:0) S(22:0); A(20:1) dS(19:0)	$C_{42}H_{83}NO_4$	25.15	$C_{48}H_{93}NO_9$	36.93	$C_{47}H_{95}N_2PO_7$	43.49
N(26:1) P(18:0); A(26:0) S(18:1); A(26:1) dS(18:0)	N(24:1) P(20:0); A(24:0) S(20:0); A(27:1) dS(18:0)		$C_{44}H_{87}NO_4$	25.22	$C_{50}H_{97}NO_9$	36.93	$C_{49}H_{99}N_2PO_7$	43.24
E(18:2) O(32:0) H(20:1)			$C_{70}H_{133}NO_6$	25.29	$C_{76}H_{143}NO_{11}$	36.76	$C_{75}H_{145}N_2PO_9$	42.11
E(18:2) O(30:0) H(20:1)			$C_{68}H_{131}NO_6$	25.41	$C_{74}H_{141}NO_{11}$	36.88	$C_{73}H_{143}N_2PO_9$	42.11
A(26:0) P(16:0)	A(25:0) P(17:0)	A(24:0) P(18:0)	$C_{42}H_{85}NO_5$	25.43	$C_{48}H_{95}NO_{10}$	36.93	$C_{47}H_{97}N_2PO_8$	43.06
E(18:2) O(31:0) H(20:1)			$C_{69}H_{131}NO_6$	25.44	$C_{75}H_{141}NO_{11}$	36.76	$C_{74}H_{143}N_2PO_9$	42.18
E(18:2) O(30:0) H(20:1)			$C_{68}H_{129}NO_6$	25.5	$C_{74}H_{139}NO_{11}$	36.88	$C_{73}H_{141}N_2PO_9$	42.18
E(18:2) O(29:0) H(20:1)			$C_{67}H_{127}NO_6$	25.55	$C_{73}H_{137}NO_{11}$	36.88	$C_{72}H_{139}N_2PO_9$	42.26
E(18:2) O(28:0) H(18:0)			$C_{64}H_{123}NO_6$	25.61	$C_{70}H_{133}NO_{11}$	36.88	$C_{69}H_{135}N_2PO_9$	42.33
N(24:1) P(16:0); A(24:0) S(16:1); A(24:1) dS(17:0)	N(20:1) P(20:0); A(20:0) S(20:0)	N(18:1) P(22:0); A(18:0) S(22:0)	$C_{40}H_{79}NO_4$	25.69	$C_{46}H_{89}NO_9$	36.93	$C_{45}H_{91}N_2PO_7$	43.72
E(18:2) O(28:0) H(20:1)			$C_{66}H_{125}NO_6$	25.73	$C_{72}H_{135}NO_{11}$	36.88	$C_{71}H_{137}N_2PO_9$	42.26
N(18:1) P(16:0); A(18:0) S(16:1); A(17:1) dS(17:0)	N(17:1) P(17:0); A(17:0) S(17:0)	N(16:1) P(18:0); N(16:0) S(18:0)	$C_{34}H_{67}N O_4$	26.31	$C_{40}H_{77}NO_9$	37.14	$C_{39}H_{79}N_2PO_7$	44.62
N(30:0) H(18:1)	N(28:0) H(20:0)	N(26:0) H(22:0)	$C_{48}H_{95}NO_4$	26.32	$C_{54}H_{105}NO_9$	36.93	$C_{53}H_{107}N_2PO_7$	43.85
N(28:0) H(19:1)	N(27:0) H(20:0)	N(26:0) H(21:0)	$C_{47}H_{93}NO_4$	26.48	$C_{53}H_{103}NO_9$	36.93	$C_{52}H_{105}N_2PO_7$	43.93

Table 3 (continued)

Identified ceramide subclasses		Ceramides		Glucosylceramides		Sphingomyelins	
		Molecular formula	RT (min)	Molecular formula	RT (min)	Molecular formula	RT (min)
N(27:0) H(18:1)	N(28:0) H(17:0)	$C_{45}H_{89}NO_4$	26.55	$C_{51}H_{99}NO_9$	36.93	$C_{50}H_{101}N_2PO_7$	43.19
N(28:0) H(18:1)	N(27:0) H(19:0)	$C_{46}H_{91}NO_4$	26.7	$C_{52}H_{101}NO_9$	36.93	$C_{51}H_{103}N_2PO_7$	43.06
N(28:0) H(16:1)	N(26:0) H(18:0)	$C_{44}H_{87}NO_4$	26.93	$C_{50}H_{97}NO_9$	36.93	$C_{49}H_{99}N_2PO_7$	43.24
N(26:0) H(16:1)	N(25:0) H(17:0)	$C_{42}H_{83}NO_4$	27.09	$C_{48}H_{93}NO_9$	36.93	$C_{47}H_{95}N_2PO_7$	43.49
N(24:0) H(16:1)	N(22:0) H(18:0)	$C_{40}H_{79}NO_4$	27.1	$C_{46}H_{89}NO_9$	36.93	$C_{45}H_{91}N_2PO_7$	43.72
N(26:0) T(16:0)	N(24:0) T(18:0)	$C_{42}H_{85}NO_5$	27.33	$C_{48}H_{95}NO_{10}$	36.93	$C_{47}H_{97}N_2PO_8$	43.06
N(18:0) H(16:1)	N(16:0) H(18:0)	$C_{34}H_{67}NO_4$	28.16	$C_{40}H_{77}NO_9$	37.14	$C_{39}H_{79}N_2PO_7$	44.62
N(17:0) H(16:1)	N(16:0) H(17:0)	$C_{33}H_{65}NO_4$	28.31	$C_{39}H_{75}NO_9$	37.22	$C_{38}H_{77}N_2PO_7$	44.62
A(36:1) H(18:1) N(36:2) T(18:0)	A(34:1) H(20:0) N(34:2) T(20:0)	$C_{54}H_{105}NO_5$	29.08	$C_{60}H_{115}NO_{10}$	37.14	Not found	
A(27:0) H(20:1) N(27:1) T(20:0)	A(26:0) H(22:0) N(26:1) T(22:0)	$C_{47}H_{93}NO_5$	29.15	$C_{53}H_{103}NO_{10}$	37.14	$C_{52}H_{105}N_2PO_8$	43.43
A(28:0) H(18:1) N(28:1) T(18:0)	A(26:0) H(20:0) N(26:1) T(20:0)	$C_{46}H_{91}NO_5$	29.64	$C_{52}H_{101}NO_{10}$	37.14	$C_{51}H_{103}N_2PO_8$	41.67
A(27:0) H(18:1) N(27:1) T(18:0)	A(26:0) H(19:0) N(26:1) T(19:0)	$C_{45}H_{89}NO_5$	29.78	$C_{51}H_{99}NO_{10}$	37.22	$C_{50}H_{101}N_2PO_8$	43.56
A(28:0) H(16:1) N(28:1) T(16:0)	A(26:0) H(18:0) N(26:1) T(18:0)	$C_{44}H_{87}NO_5$	29.84	$C_{50}H_{97}NO_{10}$	37.29	$C_{49}H_{99}N_2PO_8$	41.82
A(26:0) H(17:1) N(26:1) T(17:0)	A(24:0) H(19:0) N(24:1) T(19:0)	$C_{43}H_{85}NO_5$	29.98	$C_{49}H_{95}NO_{10}$	37.36	$C_{48}H_{97}N_2PO_8$	41.82
A(26:0) H(16:1) N(26:1) T(16:0)	A(24:0) H(18:0) N(24:1) T(18:0)	$C_{42}H_{83}NO_5$	30.04	$C_{48}H_{93}NO_{10}$	37.36	$C_{47}H_{95}N_2PO_8$	41.82
A(30:0) H(18:1) N(30:1) T(18:0)	A(28:0) H(20:0) N(28:1) T(20:0)	$C_{48}H_{95}NO_5$	30.05	$C_{54}H_{105}NO_{10}$	37.14	$C_{53}H_{107}N_2PO_8$	44.2
A(25:0) H(16:1) N(25:1) T(16:0)	A(24:0) H(17:0) N(24:1) T(17:0)	$C_{41}H_{81}NO_5$	30.33	$C_{47}H_{91}NO_{10}$	37.44	$C_{46}H_{93}N_2PO_8$	44.13
A(24:0) H(16:1) N(24:1) T(16:0)	A(23:0) H(17:0) N(23:1) T(17:0)	$C_{40}H_{79}NO_5$	30.53	$C_{46}H_{89}NO_{10}$	37.51	$C_{45}H_{91}N_2PO_8$	42.55

Table 4 Total carbon numbers of identified ceramide subclasses obtained for the RHE culture at D22. Sphingoid base moiety in columns and fatty acid moiety in lines. The newly identified subclasses of ceramide obtained for the RHE culture at D22 are colored on yellow

	S	dS	P	H	T	1-O-E_S	1-O-E_P	1-O-E_H	1-O-E_T
N	C_{41}-C_{48}	C_{41}-C_{49}	C_{34}-C_{56}	C_{33}-C_{48}	C_{44}-C_{54}		-	C_{61}-C_{66}	C_{57}-C_{60}
A	C_{34}-C_{56}	C_{34}-C_{56}	C_{42}, C_{50}, C_{52}	C_{44}-C_{54}	-	C_{64}-C_{72}	C_{58}-C_{60}	C_{58}-C_{64}	-
O	C_{52}-C_{56}	-	-	C_{50}-C_{57}	C_{50}-C_{56}	-	-	-	-
EO	C_{64}-C_{72}	-	-	C_{64}-C_{70}	-	C_{80}-C_{89}	-	C_{91}-C_{95}	C_{83}-C_{90}

(1-O-E) and on the position of ω-hydroxyl group of fatty acid with the linolenic acid (EO).

Following the nomenclature developed by Motta et al. [40] and expanded by Robson et al. [41], Masukawa et al. [42], and Rabionet [21], we suggest the following name to this subclass 1-O-E (EO) Cer.

In this new identified subclass 1-O-E (EO) Cer, three sphingoid bases were characterized: sphingosine (S), 6-hydroxysphingosine (H), or the dihydroxy-dihydro sphingosine (T). As for the fatty acid part, it is derived from the esterification of the ω-hydroxyl group of the ULC fatty acid moiety with the linoleic acid (C18:2) (EO).

In Fig. 4, we represent the characteristic fragments of 3 molecules from 3 different subclasses as explained below:

Table 5 The identified protein-bound ceramide species obtained for the RHE culture at D22. Columns 1 and 2 represent respectively the retention time and the chemical formula of the identified subclasses. The difference between the exact mass and the observed mass is shown in column 3

RT (min)	Chemical formula	△PPM (+/−)	Identified class
19.96	$C_{52}H_{99}NO_4$	2.66	OS (C52:2)
	$C_{53}H_{101}NO_4$	2.32	OS (C53:2)
	$C_{54}H_{103}NO_4$	2.6	OS (C54:2)
	$C_{55}H_{105}NO_4$	3.01	OS (C55:2)
	$C_{56}H_{107}NO_4$	3.26	OS (C56:2)
21.73	$C_{50}H_{95}NO_5$	1.97	OH (C50:2)
	$C_{51}H_{97}NO_5$	2.43	OH (C51:2)
	$C_{52}H_{99}NO_5$	2.88	OH (C52:2)
	$C_{53}H_{101}NO_5$	3.01	OH (C53:2)
	$C_{54}H_{103}NO_5$	1.93	OH (C54:2)
	$C_{55}H_{105}NO_5$	2.82	OH (C55:2)
	$C_{56}H_{107}NO_5$	2.63	OH (C56:2)
	$C_{57}H_{109}NO_5$	2.23	OH (C57:2)
22.48	$C_{50}H_{95}NO_6$	1.68	OT (C50:3)
	$C_{52}H_{99}NO_6$	1.91	OT (C52:3)
	$C_{54}H_{103}NO_6$	2.04	OT (C54:3)
	$C_{55}H_{105}NO_6$	1.6	OT (C55:3)
	$C_{56}H_{107}NO_6$	2.39	OT (C56:3)

Double esterified ceramide 1-O-E (EO)-T, ($C_{86}H_{165}NO_8$) (1-O-E (18:0) EO (18:2/32:0) T (te18:0))

In the full scan spectrum, the most intense peak was [M+H-2H_2O]^+ corresponding to m/z 1305.24. The ion [M+H]^+ at m/z 1341.26 was less intense.

In the MS^2 fragmentation of the parent ion m/z 1305.24 [M+H-2H_2O]^+, we observed a m/z 1020.97 indicating the loss of third water molecule and the acyl chain (18:0) at the 1-O-position of sphingoid [M-2H_2O-$C_{18}H_{36}O_2$]^+.

Then, in MS^3 of m/z 1020.97, we observed the m/z 756.72 related to the cleavage of the linoleic acid (18:2) esterified on

Table 6 The newly identified subclasses of ceramide obtained for the RHE culture at D22. Columns 1 and 2 represent respectively the retention time and the chemical formula of the identified subclasses. The difference between the exact mass and the observed mass is shown in column 3

RT (min)	Chemical formula	△PPM (+/−)	Identified class
18.45–20	$C_{80}H_{149}NO_6$	2.365	1-O-E(EO)S
	$C_{80}H_{151}NO_6$	2.884	
	$C_{81}H_{153}NO_6$	3.943	
	$C_{81}H_{151}NO_6$	1.884	
	$C_{82}H_{155}NO_6$	4.578	
	$C_{82}H_{153}NO_6$	1.863	
	$C_{84}H_{157}NO_6$	2.53	
	$C_{89}H_{167}NO_6$	3.68	
	$C_{91}H_{173}NO_7$	0.766	1-O-E(EO)H
	$C_{92}H_{175}NO_7$	3.15	
	$C_{93}H_{177}NO_7$	2.78	
	$C_{94}H_{179}NO_7$	4.9	
	$C_{94}H_{177}NO_7$	3.09	
	$C_{95}H_{179}NO_7$	4.04	
	$C_{83}H_{159}NO_8$	5.332	1-O-E(EO)T
	$C_{84}H_{161}NO_8$	5.321	
	$C_{85}H_{163}NO_8$	4.88	
	$C_{86}H_{165}NO_8$	3.26	
	$C_{87}H_{167}NO_8$	7.05	
	$C_{88}H_{169}NO_8$	4.76	
	$C_{90}H_{173}NO_8$	4.9	

the ω-hydroxyl group of ceramide ultra-long chain fatty acid of ceramide $[M-2H_2O-C_{18}H_{37}O_2-C_{18}H_{32}O]^+$ and the m/z 738.71 due to one water molecule loss.

Finally, we observed the peak of the fatty acid moiety at m/z 494.49 $[CHO-C_{30}H_{60}CO-NH_3]^+$ and the sphingoid base moiety without its hydroxyl groups at m/z 262.28 $[C_{11}H_{23}-CH=CH-CH=C=CH-C(CH2)-NH3]^+$ (Fig. 4a).

Double esterified ceramide 1-O-E (EO)-S, ($C_{84}H_{157}NO_6$), 1-O-E (16:1) EO(18:2/30:0) S (d20:1)

In the full scan spectrum, the most intense peak was $[M+H]^+$ at m/z 1277.21.

In the MS^2 fragmentation of the parent ion m/z 1277.21 $[M+H]^+$, we observed a m/z 1004.97 indicating the loss of one water molecule and the acyl chain (16:1) at the 1-O-position of sphingoid $[M-H_2O-C_{16}H_{30}O_2]^+$.

Then, in MS^3 of m/z 1004.97, we observed the m/z 740.73 corresponding to the cleavage of the linoleic acid (18:2) esterified on the ω-hydroxyl group of ceramide ultra-long chain fatty acid of ceramide $[M-H_2O-C_{16}H_{30}O_2-C_{18}H_{32}O]^+$.

Finally, we observed the peak of the fatty acid moiety $[CHO-C_{28}H_{56}CO-NH_3]^+$ and the sphingoid base moiety after one water molecule loss $[C_{15}H_{31}-CH=C=CH-C(CH_2)-NH_3]^+$ at m/z 466.46 and 292.30 respectively (Fig. 4b).

Double esterified ceramide 1-O-E (EO)-H, ($C_{92}H_{175}NO_7$), 1-O-E (24:0) EO (18:2/32:0) H (t18:1)

In the full scan spectrum, the most intense peak was $[M+H-H_2O]^+$ matching m/z 1389.33. The ion $[M+H]^+$ at m/z 1407.34 was less intense.

In the MS^2 fragmentation of the parent ion m/z 1389.33 $[M+H-H_2O]^+$, we observed a m/z 1020.97 indicating the loss
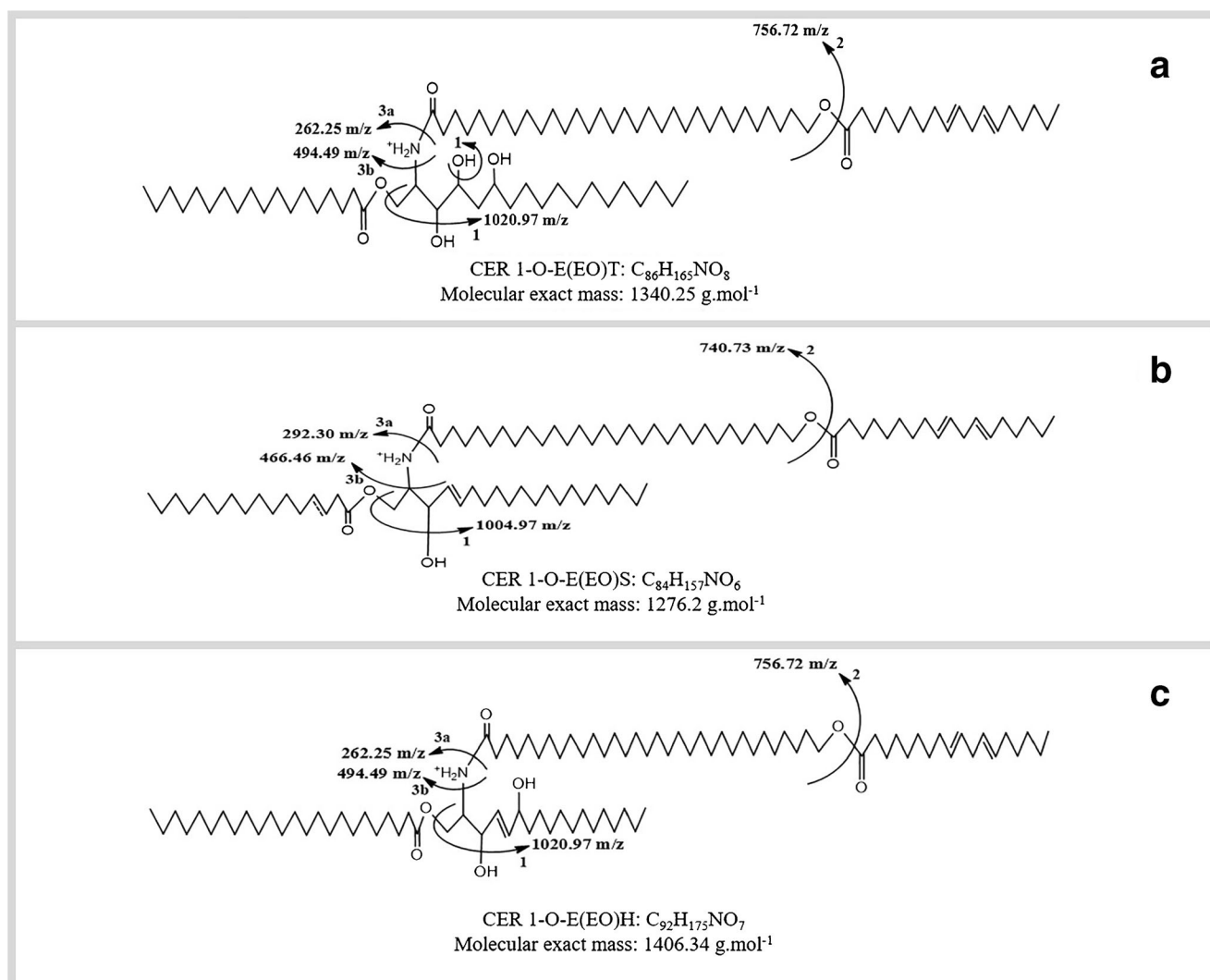

Fig. 4 The fragmentation observed in full scan and MS^2 spectra of the new ceramide subclass 1-O-E(EO) Cer: **a** 1-O-E(EO)T, **b** 1-O-E(EO)S, **c** 1-O-E(EO)H

of one water molecule and the acyl chain (24:0) at the 1-O-position of sphingoid $[M-H_2O-C_{24}H_{48}O_2]^+$.

Then, in MS^3 of m/z 1020.97, we observed the m/z 756.72 corresponding to the cleavage of the linoleic acid (18:2) esterified on the ω-hydroxyl group of ceramide ultra-long chain fatty acid of ceramide $[M-H_2O-C_{24}H_{48}O_2-C_{18}H_{32}O]^+$ and the m/z 738.71 due to the loss of the second water molecule.

Finally, we observed the peak of the fatty acid moiety $[CHO-C_{30}H_{60}CO-NH_3]^+$ at m/z 494.49 and the sphingoid base moiety $[C_{11}H_{23}-CH=CH-CH=C=CH-C(CH2)-NH3]^+$ at m/z 262.28 after two water molecule losses (Fig. 4c).

Discussion

The aim of this study was to investigate at the molecular level the overall epidermis lipidome, especially the biomarkers of keratinocyte differentiation: ceramides, glucosylceramides, and sphingomyelins. Indeed, studying lipid biosynthesis as well as the lipids from the *stratum corneum* helps us to explain the impaired barrier function induced by metabolic pathways disruption.

To this end, a new analytical approach in NPLC/HR-MS^n was developed herein to permit the simultaneous characterization of epidermis lipids.

The complexity of lipids mixture represents a real analytical challenge. Epidermis lipids consist of 9 lipid classes (TG, DG, MG, Chol, FFA, Cer, GlcCer, SM, and PL) and 18 subclasses of ceramides, with a large polarity range. In addition, within each class or subclass, the structures are very diversified.

Thus, our analytical protocol allowed us to separate correctly all epidermis lipid classes according to the polar head, while preserving the structural integrity of molecules, by starting from the less polar molecules the triglycerides until the more polar the sphingomyelins in one single run. In fact, the ceramide class is divided into different subclasses in form of several peaks between 18.3 and 30 min, which differ by the structural microheterogeneity, due to the number of hydroxylation, the number of instauration, the chain length of amide-linked fatty acid, and the isomeric. However, for glucosylceramides and sphingomyelines, all the lipids of each class are eluted in a single chromatographic peak at 36.9 min and 43.1 min respectively, because the polarities of the glucosyl and phosphocholine groups are greater than the polarity differences induced by their under-class structural microheterogeneity.

Additionally, the use of high-resolution mass spectrometry to determine the exact mass of molecules and the optimization of the fragmentation parameters enabled us to identify and to determine the microstructure within the ceramide subclasses in the reconstructed human epidermis (RHE). Full scan and MS^2 spectra were explained and illustrated for the three biomarkers of interest: ceramides, glucosylceramides, and sphingomyelins. Thus, we were able to determine the subclass and the number of water losses corresponding to the numbers of the hydroxyl groups of the polar head and to obtain precise information on the lengths of the alkyl chains as well as the number of unsaturation of the acid part and the sphingoid part.

In the literature, several methods were developed to analyze ceramides in detail in order to study only the *stratum corneum*, the upper layer of epidermis, but they do not take into consideration the totality of epidermis layers [7, 8, 43, 44]. Other studies reported the analysis of lipid mixtures using the separation by class in normal-phase liquid chromatography coupled with high-resolution mass spectrometry. Nevertheless, the elution gradient was not adapted to epidermis lipids especially to discriminate ceramide subclasses following the increasing polarity and to separate sphingomyelins from phospholipids [15, 30, 32]. In addition, the epidermal lipids are subjected of wide isomeric phenomenon, i.e., different molecules can have the same molecular formula but belong to two lipid subclasses coming from two different metabolic pathways. Thus, the characterization of the fine structure of biomarkers is crucial to be able to follow and to study the metabolic pathways. In summary, using a unique analysis, we have gathered the advantages of two types of methods: those able to analyze a wide range of compounds and those offering a precise characterization by molecular species [29, 43, 45, 46]. This lipidomic approach will permit the comparison of epidermis lipid profiles between several samples in order to identify the eventual markers of a physio-pathologic status.

The identified compounds within the RHE represent the overall classes of skin CERs: long, very long, and ultra-long chain CERs (NS, NdS, NP, NH, NT, AS, AdS, AP, AH); esterified ultra-long chain CERs, which are esterified either with linoleic acid (EOH, EOS) or with cornified envelope proteins and are required for the water permeability barrier (OS, OH, OT) and 1-O-acylceramides (EAH, ENT, EAP). Thus, we would be able to characterize overall ceramide subclasses in the epidermis according to the literature, including the ceramide subclasses which are present at low proportions in the *stratum corneum*, such as the NT and OT. This requires a significant sensitivity of the analytical method to detect these molecules and to demonstrate the advantage of our analysis protocol.

In the present study, a new ceramide subclass was characterized in the RHE sample. We suggest the following nomenclature for it: 1-O-E (EO) Cer. These ceramides are double esterified: on the 1-O-position of sphingoid base with a long to a very long chain acyl residues (1-O-E) and on the position of ω-hydroxyl group of fatty acid with the linolenic acid (EO). To our knowledge, so far, it has been shown that during epidermis ceramide biosynthesis, the 1-O-acylceramides (1-O-AcylCers) subclass is generated by the 1-O-Acyl esterification of an alkyl chain to the primary hydroxyl in position 1 of the sphingoid base (1-O-E). Only two 1-O-acylceramides

(1-O-AcylCers) subclasses have been identified in the literature: 1-O-ENS and 1-O-EAS ceramides. In these cases, the sphingoid base is the sphingosine (S), and on the fatty acid part, the acyl chain is a non-hydroxy (N) or α-hydroxy (A) [21]. In the new identified subclass 1-O-E (EO) Cer, three sphingoid bases were characterized: sphingosine (S), 6-hydroxysphingosine (H), or the dihydroxy-dihydro sphingosine (T), and fatty acid part is derived from the esterification of the ω-hydroxyl group of the ULC fatty acid moiety with the linoleic acid (C18:2) (EO) (Table 6). The identification of this new class leads to suggest a novel biosynthetic pathway in which 1-O-Acyl esterification could be done on ω-hydroxy-ultra long chain-ceramide before the step of glycosylation on the Golgi apparatus. Indeed, regarding the chemical structure and the hydrophobicity of this class, its role in the barrier function seems to be very important to explore. Moreover, the mechanism already illustrated of ω-hydroxy-ultra long chain-ceramide ester bound to glutamate residues of the proteins (mostly involucrin) at the surface of a corneocyte [47] to establish the barrier function could be possible to transpose on the 1-O-E (EO) Cer. In addition, the chain length could have an impact on lipid organization if they are present at *stratum corneum* level and also participate in the barrier function.

At the level of biomarkers of keratinocyte differentiation, the same ceramide subclasses identified within RHE sample have been characterized in glucosylceramide and sphingomyelin classes. A previous study mentioned that GlcCER species are predominant in epidermis ceramides, being precursors for non-h-ceramides (N: NS, NH, NP), α-h-ceramides (A: AS, AH, AP), and all ω-esterified (EO: EOS, EOH, EOP) and protein-bound ceramide species (O: OS, OH) [21, 48]. SM are precursors for exclusively sphingosine-containing NS- and AS-ceramides [20, 21]. Hence, the lack of sphingomyelinase results in a milder compromised barrier as compared with barrier disruption in the case of β-glucocerebrosidase deficiency [21, 49]. Interestingly, in this work and for the first time, studying the totality of epidermis lipids allowed us to characterize several new sphingomyelin subclasses: NS, NdS, NP, NH, NT, AH, AdS, AS, AP, EOS, EOH (Table 3). Thus, we assume that the lack of sphingomyelinase could cause significant disruption to the barrier function. These observations show the possibility and the importance of following lipid biosynthesis simultaneously in each epidermis layer and highlight the relevance of our method at different levels: sample preparation, chromatographic separation, detection, and molecular characterization.

Finally, the analytical method described herein is adapted to the analysis of epidermis lipids in particular. We have established an approach which is well adapted for the complexity of these lipids and can be widely exploited in lipidomic studies with a direct access to the biomarkers of

interest within the cosmetic and dermato-pharmaceutical investigations.

Compliance with ethical standards

References

1. Breiden B, Gallala H, Doering T, Sandhoff K. Optimization of submerged keratinocyte cultures for the synthesis of barrier ceramides. Eur J Cell Biol. 2007;86(11–12):657–73.

2. Franzke CW, Cobzaru C, Triantafyllopoulou A, Loffek S, Horiuchi K, Threadgill DW, et al. Epidermal ADAM17 maintains the skin barrier by regulating EGFR ligand-dependent terminal keratinocyte differentiation. J Exp Med. 2012;209(6):1105–19.

3. van Drongelen V, Alloul-Ramdhani M, Danso MO, Mieremet A, Mulder A, van Smeden J, et al. Knock-down of filaggrin does not affect lipid organization and composition in stratum corneum of reconstructed human skin equivalents. Exp Dermatol. 2013;22(12):807–12.

4. Vyumvuhore R, Tfayli A, Duplan H, Delalleau A, Manfait M, Baillet-Guffroy A. Effects of atmospheric relative humidity on stratum corneum structure at the molecular level: ex vivo Raman spectroscopy analysis. Analyst. 2013;138(14):4103–11.

5. Sahle FF, Gebre-Mariam T, Dobner B, Wohlrab J, Neubert RH. Skin diseases associated with the depletion of stratum corneum lipids and stratum corneum lipid substitution therapy. Skin Pharmacol Physiol. 2015;28(1):42–55.

6. Mlitz V, Latreille J, Gardinier S, Jdid R, Drouault Y, Hufnagl P, et al. Impact of filaggrin mutations on Raman spectra and biophysical properties of the stratum corneum in mild to moderate atopic dermatitis. J Eur Acad Dermatol Venereol. 2012;26(8):983–90.

7. van Smeden J, Bouwstra JA. Stratum corneum lipids: their role for the skin barrier function in healthy subjects and atopic dermatitis patients. Curr Probl Dermatol. 2016;49:8–26.

8. van Smeden J, Hoppel L, van der Heijden R, Hankemeier T, Vreeken RJ, Bouwstra JA. LC/MS analysis of stratum corneum lipids: ceramide profiling and discovery. J Lipid Res. 2011;52(6): 1211–21.

9. Mizutani Y, Mitsutake S, Tsuji K, Kihara A, Igarashi Y. Ceramide biosynthesis in keratinocyte and its role in skin function. Biochimie. 2009;91(6):784–90.

10. Arct J, Majewski S, Leleń-Kamińska K, Stepulak M, Malejczyk M. Biological activity of ceramides and other sphingolipids. Postep Derm Alergol. 2012;29(3/2012):169–75.

11. Holleran WM, Takagi Y, Uchida Y. Epidermal sphingolipids: metabolism, function, and roles in skin disorders. FEBS Lett. 2006;580(23):5456–66.

12. Brooks G, Idson B. Skin lipids. Int J Cosmet Sci. 1991;13(2):103–13.

13. Farwanah H, Wohlrab J, Neubert RH, Raith K. Profiling of human stratum corneum ceramides by means of normal phase LC/APCI-MS. Anal Bioanal Chem. 2005;383(4):632–7.

14. van Smeden J, Janssens M, Gooris GS, Bouwstra JA. The important role of stratum corneum lipids for the cutaneous barrier function. Biochim Biophys Acta. 2014;1841(3):295–313.

15. Graeve M, Janssen D. Improved separation and quantification of neutral and polar lipid classes by HPLC-ELSD using a monolithic silica phase: application to exceptional marine lipids. J Chromatogr B Anal Technol Biomed Life Sci. 2009;877(20–21):1815–9.

16. Gerits LR, Pareyt B, Delcour JA. Single run HPLC separation coupled to evaporative light scattering detection unravels wheat flour endogenous lipid redistribution during bread dough making. LWT Food Sci Technol. 2013;53(2):426–33.

17. Homan R, Anderson MK. Rapid separation and quantitation of combined neutral and polar lipid classes by high-performance liquid chromatography and evaporative light-scattering mass detection. J Chromatogr B Biomed Sci Appl. 1998;708(1):21–6.

18. Cajka T, Fiehn O. Comprehensive analysis of lipids in biological systems by liquid chromatography-mass spectrometry. TrAC Trends Anal Chem. 2014;61:192–206.

19. Holleran WM, Takagi Y, Menon GK, Legler G, Feingold KR, Elias PM. Processing of epidermal glucosylceramides is required for optimal mammalian cutaneous permeability barrier function. J Clin Invest. 1993;91(4):1656–64.

20. Uchida Y, Hara M, Nishio H, Sidransky E, Inoue S, Otsuka F, et al. Epidermal sphingomyelins are precursors for selected stratum corneum ceramides. J Lipid Res. 2000;41(12):2071–82.

21. Rabionet M, Gorgas K, Sandhoff R. Ceramide synthesis in the epidermis. Biochim Biophys Acta. 2014;1841(3):422–34.

22. Bouwstra JA, Ponec M. The skin barrier in healthy and diseased state. Biochim Biophys Acta. 2006;1758(12):2080–95.

23. t'Kindt R, Jorge L, Dumont E, Couturon P, David F, Sandra P, et al. Profiling and characterizing skin ceramides using reversed-phase liquid chromatography-quadrupole time-of-flight mass spectrometry. Anal Chem. 2012;84(1):403–11.

24. Schmitt T, Neubert RHH. State of the art in stratum corneum research: the biophysical properties of ceramides. Chem Phys Lipids. 2018;216:91–103.

25. Guillard E, Tfayli A, Manfait M, Baillet-Guffroy A. Thermal dependence of Raman descriptors of ceramides. Part II: effect of chains lengths and head group structures. Anal Bioanal Chem. 2011;399(3):1201–13.

26. Jennemann R, Rabionet M, Gorgas K, Epstein S, Dalpke A, Rothermel U, et al. Loss of ceramide synthase 3 causes lethal skin barrier disruption. Hum Mol Genet. 2012;21(3):586–608.

27. Coderch L, Lopez O, de la Maza A, Parra JL. Ceramides and skin function. Am J Clin Dermatol. 2003;4(2):107–29.

28. Marekov LN, Steinert PM. Ceramides are bound to structural proteins of the human foreskin epidermal cornified cell envelope. J Biol Chem. 1998;273(28):17763–70.

29. Rabionet M, Bayerle A, Marsching C, Jennemann R, Grone HJ, Yildiz Y, et al. 1-O-acylceramides are natural components of human and mouse epidermis. J Lipid Res. 2013;54(12):3312–21.

30. Imbert L, Gaudin M, Libong D, Touboul D, Abreu S, Loiseau PM, et al. Comparison of electrospray ionization, atmospheric pressure chemical ionization and atmospheric pressure photoionization for a lipidomic analysis of Leishmania donovani. J Chromatogr A. 2012;1242:75–83.

31. Hvattum E, Uran S, Sandbaek AG, Karlsson AA, Skotland T. Quantification of phosphatidylserine, phosphatidic acid and free fatty acids in an ultrasound contrast agent by normal-phase high-performance liquid chromatography with evaporative light scattering detection. J Pharm Biomed Anal. 2006;42(4):506–12.

32. Abreu S, Solgadi A, Chaminade P. Optimization of normal phase chromatographic conditions for lipid analysis and comparison of associated detection techniques. J Chromatogr A. 2017;1514:54–71.

33. Ramos RG, Libong D, Rakotomanga M, Gaudin K, Loiseau PM, Chaminade P. Comparison between charged aerosol detection and light scattering detection for the analysis of Leishmania membrane phospholipids. J Chromatogr A. 2008;1209(1–2):88–94.

34. Zheng L, T'Kind R, Decuypere S, von Freyend SJ, Coombs GH, Watson DG. Profiling of lipids in Leishmania donovani using hydrophilic interaction chromatography in combination with Fourier transform mass spectrometry. Rapid Commun Mass Spectrom. 2010;24(14):2074–82.

35. Christie WW. Rapid separation and quantification of lipid classes by high performance liquid chromatography and mass (light-scattering) detection. J Lipid Res. 1985;26(4):507–12.

36. Postle AD, Wilton DC, Hunt AN, Attard GS. Probing phospholipid dynamics by electrospray ionisation mass spectrometry. Prog Lipid Res. 2007;46(3–4):200–24.

37. Folch J, Ascoli I, Lees M, Meath JA, Le BN. Preparation of lipide extracts from brain tissue. J Biol Chem. 1951;191(2):833–41.

38. Folch J, Lees M, Sloane Stanley GH. A simple method for the isolation and purification of total lipides from animal tissues. J Biol Chem. 1957;226(1):497–509.

39. Bligh EG, Dyer WJ. A rapid method of total lipid extraction and purification. Can J Biochem Physiol. 1959;37(8):911–7.

40. Motta S, Monti M, Sesana S, Caputo R, Carelli S, Ghidoni R. Ceramide composition of the psoriatic scale. Biochim Biophys Acta. 1993;1182(2):147–51.

41. Robson KJ, Stewart ME, Michelsen S, Lazo ND, Downing DT. 6-Hydroxy-4-sphingenine in human epidermal ceramides. J Lipid Res. 1994;35(11):2060–8.

42. Masukawa Y, Narita H, Shimizu E, Kondo N, Sugai Y, Oba T, et al. Characterization of overall ceramide species in human stratum corneum. J Lipid Res. 2008;49(7):1466–76.

43. Boiten W, Helder R, van Smeden J, Bouwstra J. Selectivity in cornified envelop binding of ceramides in human skin and the role of LXR inactivation on ceramide binding. Biochim Biophys Acta Mol Cell Biol Lipids. 2019;1864(9):1206–13.

44. van Smeden J, Boiten WA, Hankemeier T, Rissmann R, Bouwstra JA, Vreeken RJ. Combined LC/MS-platform for analysis of all major stratum corneum lipids, and the profiling of skin substitutes. Biochim Biophys Acta. 2014;1841(1):70–9.

45. Cha HJ, He C, Zhao H, Dong Y, An IS, An S. Intercellular and intracellular functions of ceramides and their metabolites in skin (review). Int J Mol Med. 2016;38(1):16–22.

46. Vávrová K, Kováčik A, Opálka L. Ceramides in the skin barrier. Eur Pharm J. 2017;64 (2):28–35.

47. Candi E, Schmidt R, Melino G. The cornified envelope: a model of cell death in the skin. Nat Rev Mol Cell Biol. 2005;6(4):328–40.

48. Hamanaka S, Suzuki A, Hara M, Nishio H, Otsuka F, Uchida Y. Human epidermal glucosylceramides are major precursors of stratum corneum ceramides. J Investig Dermatol. 2002;119(2):416–23.

49. Schmuth M, Man M-Q, Weber F, Gao W, Feingold KR, Fritsch P, et al. Permeability barrier disorder in Niemann–Pick disease: sphingomyelin–ceramide processing required for normal barrier homeostasis. J Investig Dermatol. 2000;115(3):459–66.